Linear and nonlinear quantum Zeno and anti-Zeno effects in a nonlinear optical coupler

Kishore Thapliyal[a], Anirban Pathak[a,*], and Jan Peřina[b,c]

[a] *Jaypee Institute of Information Technology, A-10, Sector-62, Noida, UP-201307, India*
[b] *RCPTM, Joint Laboratory of Optics of Palacky University and Institute of Physics of Academy of Science of the Czech Republic, Faculty of Science, Palacky University, 17. listopadu 12, 771 46 Olomouc, Czech Republic*
[c] *Department of Optics, Palacky University, 17. listopadu 12, 771 46 Olomouc, Czech Republic*

arXiv:1511.02317v1 [quant-ph] 7 Nov 2015

Quantum Zeno and anti-Zeno effects are studied in a symmetric nonlinear optical coupler, which is composed of two nonlinear ($\chi^{(2)}$) waveguides that are interacting with each other via the evanescent waves. Both the waveguides operate under second harmonic generation. However, to study quantum Zeno and anti-Zeno effects one of them is considered as the system and the other one is considered as the probe. Considering all the fields involved as weak, a completely quantum mechanical description is provided, and the analytic solutions of Heisenberg's equations of motion for all the field modes are obtained using a perturbative technique. Photon number statistics of the second harmonic mode of the system is shown to depend on the presence of the probe, and this dependence is considered as quantum Zeno and anti-Zeno effects. Further, it is established that as a special case of the momentum operator for $\chi^{(2)}-\chi^{(2)}$ symmetric coupler we can obtain momentum operator of $\chi^{(2)}-\chi^{(1)}$ asymmetric coupler with linear ($\chi^{(1)}$) waveguide as the probe, and in such a particular case, the expressions obtained for Zeno and anti-Zeno effects with nonlinear probe (which we referred to as nonlinear quantum Zeno and anti-Zeno effects) may be reduced to the corresponding expressions with linear probe (which we referred to as the linear quantum Zeno and anti-Zeno effects). Linear and nonlinear quantum Zeno and anti-Zeno effects are rigorously investigated, and it is established that in the stimulated case, we may switch between quantum Zeno and anti-Zeno effects just by controlling the phase of the second harmonic mode of the system or probe.

PACS numbers:
Keywords:

I. INTRODUCTION

In the 5th century BC, the Greek philosopher Zeno of Elea introduced a set of paradoxes of motion. These paradoxes, which are now known as Zeno's paradoxes, were unsolved for long, and they fascinated mathematicians, logicians, physicists and other creative minds since their introduction. In the recent past, a quantum analogue of Zeno's paradoxes has been studied intensively. Specifically, in the late 50s and early 60s of the 20th century, Khalfin studied nonexponential decay of unstable atoms [1]. Later on, in 1977, Misra and Sudarshan [2] showed that under continuous measurement, an unstable particle will never be found to decay, and in analogy with classical Zeno's paradox they named this phenomenon as *Zeno's quantum paradox*. Quantum Zeno effect (QZE) in the original formulation refers to the inhibition of the temporal evolution of a system on continuous measurement [2], while quantum anti-Zeno effect (QAZE) or inverse Zeno effect refers the enhancement of the evolution instead of the inhibition (see Refs. [3–5] for the reviews). Here, it is important to note that usually quantum Zeno effect is viewed as a process, which is associated with the repeated projective measurement. This is only a specific manifestation of quantum Zeno effect. In fact, it can be manifested in a few equivalent ways [6]. One such manifestation of quantum Zeno effect is a process in which continuous interaction between the system and probe leads to quantum Zeno effect. Here, we aim to study the continuous interaction type manifestation of quantum Zeno effect in a symmetric nonlinear optical coupler, which is made of two nonlinear waveguides with $\chi^{(2)}$ nonlinearity, and each of the waveguides is operating under second harmonic generation. As we are describing an optical coupler, the waveguides are coupled with each other. More precisely, these two waveguides interact with each other through the evanescent waves. We consider one of the waveguides as the probe and the other one as the system. In what follows, we will show that the beauty of the symmetric nonlinear optical coupler ($\chi^{(2)}-\chi^{(2)}$ coupler) studied here is that the results obtained for this coupler can be directly reduced to the corresponding results for an asymmetric nonlinear optical coupler where the probe is linear ($\chi^{(1)}$) and the system is nonlinear ($\chi^{(2)}$). We have reported quantum Zeno and anti-Zeno effects in both the symmetric ($\chi^{(2)}-\chi^{(2)}$) nonlinear optical coupler and asymmetric ($\chi^{(2)}-\chi^{(1)}$) nonlinear optical coupler. Following an earlier work [7], we refer to the Zeno effect observed due to the continuous interaction of a nonlinear $\left(\chi^{(2)}\right)$ probe as the nonlinear Zeno effect. Similarly, the Zeno effect observed due to the continuous interaction of a linear $\left(\chi^{(1)}\right)$ probe is referred to as the linear Zeno effect.

Optical couplers can be prepared easily and several exciting applications of the optical couplers have been reported in the recent past (see [8–10] and references therein). Consequently, it is no wonder that quantum Zeno and anti-Zeno effects have been investigated in various types of optical couplers [11–15]. Specifically, quantum Zeno and anti-Zeno effects were shown in Raman and Brillouin scattering using a ($\chi^{(3)}-\chi^{(1)}$) asymmetric nonlinear optical coupler [12]; their existence was also

*Email: anirban.pathak@gmail.com, Phone: +91 9717066494

shown in the $\chi^{(2)}-\chi^{(1)}$ optical couplers [13], $\chi^{(2)}-\chi^{(2)}$ optical couplers [14], etc. In all these studies, it was always considered that one of the mode in the nonlinear waveguide (this waveguide is considered as the system) is coupled with the auxiliary mode in a (non)linear waveguide (this waveguide is considered as the probe). Actually, the auxiliary mode acts as the probe since its coupling with the system implements continuous observation on the evolution of the system (nonlinear waveguide) and changes the photon statistics of the other modes (which are not coupled to the probe mode) of the nonlinear waveguide. Quantum Zeno and anti-Zeno effects have also been investigated in optical systems other than couplers, such as in parametric down-conversion [16–18], parametric down conversion with losses [19], an arrangement of beam splitters [20], etc. In these studies on quantum Zeno effect in optical systems, often the pump mode has been considered strong, and thus the complexity of a completely quantum mechanical treatment has been circumvented. Keeping this in mind, here we plan to use a completely quantum mechanical description of the coupler.

Initially, interest in quantum Zeno effect was theoretical and purely academic in nature, but with time quantum Zeno effect has been experimentally realized by several groups using different techniques [21–23]. Not only that, several interesting applications of quantum Zeno effect have also been proposed [21, 24–27]. Specifically, in Refs. [26, 27], it was established that the quantum Zeno effect may be used to increase the resolution of absorption tomography. A few of the proposed applications have also been experimentally realized. For example, Kwait et al. implemented high-efficiency quantum interrogation measurement using quantum Zeno effect [21]. Until recently, all the investigations related to the quantum Zeno effect were restricted to the microscopic world. Recently, in a very interesting work, it has been extended to the macroscopic world by showing the evidence for the existence of quantum Zeno effect for large black holes [28]. Possibility of observing the macroscopic Zeno effect was also studied in the context of stationary flows in nonlinear waveguides with localized dissipation [29]. The interest in quantum Zeno effect has recently been amplified with the advent of various protocols of quantum communication that are based on quantum Zeno effect. Specifically, in Ref. [25], a counterfactual protocol of direct quantum communication was proposed using chained quantum Zeno effect, and in Ref. [24], the same effect is used to propose a scheme for counterfactual quantum computation. In the past, a proposal for quantum computing was made using an environment induced quantum Zeno effect to confine the dynamics in a decoherence-free subspace [30]. Recently, quantum Zeno effect has also been used to reduce communication complexity [31]. These applications of quantum Zeno effect and easy production of optical couplers motivated us to systematically investigate the possibility of observing quantum Zeno and anti-Zeno effects in a symmetric nonlinear coupler which is not studied earlier using a completely quantum description.

To investigate the existence of quantum Zeno and anti-Zeno effects in the optical coupler of our interest, we have obtained closed form analytic expressions for the spatial evolution of the different field operators using the Sen-Mandal perturbative approach [8, 9, 32], which is known to produce better results compared to the usual short-length approximation method [33]. Actually, in sharp contrast to the short length approximated solutions, the solutions of Heisenberg's equations of motion obtained using the Sen-Mandal approach are not restricted by length. This is why we use Sen-Mandal perturbative approach and a completely quantum mechanical description of the coupler for our investigation. In the past, photon statistics and dynamics of the symmetric coupler of our interest was studied by some of the present authors with an assumption that both the second harmonic modes are strong [34]. The assumption circumvented the use of completely quantum mechanical description. Further, the system has also been used to model a beam splitter with second order nonlinearity [35]. Present investigation, not only revealed the existence of nonlinear quantum Zeno and anti-Zeno effects it also established the existence of linear Zeno and anti-Zeno effects. The study also showed that switching between quantum Zeno and anti-Zeno effects is possible by varying phase-mismatches.

The rest of the paper is organized as follows. In Section II, we briefly describe the momentum operator for the symmetric nonlinear optical coupler and the method used here to obtain the analytic expressions of the spatial evolution of the field operators of various modes. However, the detailed solution obtained here is shown in the Appendix A. In Section III, the existence of quantum Zeno and anti-Zeno effects are systematically investigated. Finally the paper is concluded in Section IV.

II. SYSTEM AND SOLUTION

Momentum operator of a symmetric nonlinear optical coupler, prepared by combining two nonlinear (quadratic) waveguides operated by second harmonic generation (as shown in Fig. 1 a), in interaction picture is given by [36]

$$\begin{aligned} G_{\rm sym} &= \hbar k a_1 b_1^\dagger + \hbar\Gamma_a a_1^2 a_2^\dagger \exp(i\Delta k_a z) \\ &+ \hbar\Gamma_b b_1^2 b_2^\dagger \exp(i\Delta k_b z) + \text{H.c.}\,, \end{aligned} \tag{1}$$

where the annihilation (creation) operators a_i ($a_i^\dagger$) and b_i ($b_i^\dagger$) correspond to the field operators in two nonlinear waveguides. Here, $a_1(k_{a_1})$ and $a_2(k_{a_2})$ denote annihilation operators (wave vectors) for fundamental and second harmonic modes, respectively, in one waveguide. Similarly, $b_1(k_{b_1})$ and $b_2(k_{b_2})$ represent annihilation operators (wave vectors) for fundamental and second harmonic modes, respectively, in second waveguide. Further, H.c. stands for the Hermitian conjugate; $\Delta k_j = |2k_{j_1} - k_{j_2}|$ refers to the phase mismatch between the fundamental and second harmonic beams; the parameters k and Γ_j denote the linear and nonlinear coupling constants, respectively, where $j \in \{a, b\}$. The momentum operator described above is completely quantum mechanical in the sense that all the modes involved in the process are considered weak and treated quantum mechanically. Thus, we consider pump as weak and note that $\Gamma_j \ll k$ as k and Γ_j are

proportional to the linear ($\chi^{(1)}$) and nonlinear ($\chi^{(2)}$) susceptibilities, respectively and usually $\chi^{(2)}/\chi^{(1)} \simeq 10^{-6}$.

For the study of quantum Zeno and anti-Zeno effects in a system we need a system momentum operator with a continuous interaction with a probe. In this particular system, the symmetric nonlinear optical coupler, we can consider that the system, which is described by $G_{\rm sys} = \hbar\Gamma_b b_1^2 b_2^\dagger \exp(i\Delta k_b z) + {\rm H.c.}$, is in continuous interaction with the probe, which is described by $G_{\rm probe} = \hbar k a_1 b_1^\dagger + \hbar\Gamma_a a_1^2 a_2^\dagger \exp(i\Delta k_a z) + {\rm H.c.}$. Here, the probe itself is considered to be nonlinear. Further, if we take $\Gamma_a = 0$ in Eq. (1), i.e., if we consider probe to be linear, we obtain [8, 9, 32]

$$G_{\rm asym} = \hbar k a b_1^\dagger + \hbar\Gamma b_1^2 b_2^\dagger \exp(i\Delta k z) + {\rm H.c.}\,, \qquad (2)$$

which is the momentum operator of an asymmetric nonlinear optical coupler in the interaction picture.

The spatial evolution of various modes involved in the momentum operators (1-2) can be obtained as the simultaneous solutions of the Heisenberg's equations of motion corresponding to each mode. However, for the complex systems, such as considered here, the closed form analytic solutions are possible only by using some perturbative methods. Here, we use Sen-Mandal perturbative method [8, 9, 13, 32], which has already been shown to be superior to the frequently used short-length/time method [12, 33]. In fact, the solutions obtained using the short-length perturbative technique can be obtained as a limiting case of a solution obtained using Sen-Mandal approach. Specifically, it may be obtained by neglecting higher power terms in length, from the solutions of the Sen-Mandal method. Actually, in Sen-Mandal approach, potential solutions of the Heisenberg equations of motion for different field modes are systematically constructed. The assumed solution for the evolution of annihilation operator of a field mode is constructed in such a way that it contains all the possible higher power terms in length, but higher power terms in weak coupling constant are neglected (for detail see [8, 9, 13, 32]). As the solutions obtained using Sen-Mandal method is applicable to relatively large interaction lengths and it contains several higher power terms that are neglected in conventional short-length approach, it provides more accurate solution compared to the short-length solutions. Further, the solution obtained using Sen-Mandal method is often found successful in detecting nonclassical character of a physical system that are not detected by conventional short-length/time solution [12, 33]. Keeping these facts in mind, here we use Sen-Mandal method to obtain spatial evolution of all the field operators involved in (1). However, the closed form analytic expresseion for the spatial evolution in b_2 mode, i.e., $b_2(z)$ is provided in Appendix A. In the Appendix A, we restrict our description to $b_2(z)$ as only the coefficeints appear in the analytic expression of $b_2(z)$ appear in the expressions of linear and nonlinear Zeno parameters. Specifically, Heisenberg's equations of motion for different field modes involved in the momentum operator (1) are obtained in Eq. (A.1) in Appendix A. The closed form analytic expressions for the spatial evolution of all the field modes up to quadratic terms in nonlinear coupling constants (Γ_j) are subsequently obtained using Sen-Mandal perturbation method (cf. Suuplementary material for all modes and Appendix A for b_2 modes). In what follows, we use the expression of $b_2(z)$ provided in Appendix A to investigate the linear and nonlinear Zeno and anti-Zeno effects in the optical couplers.

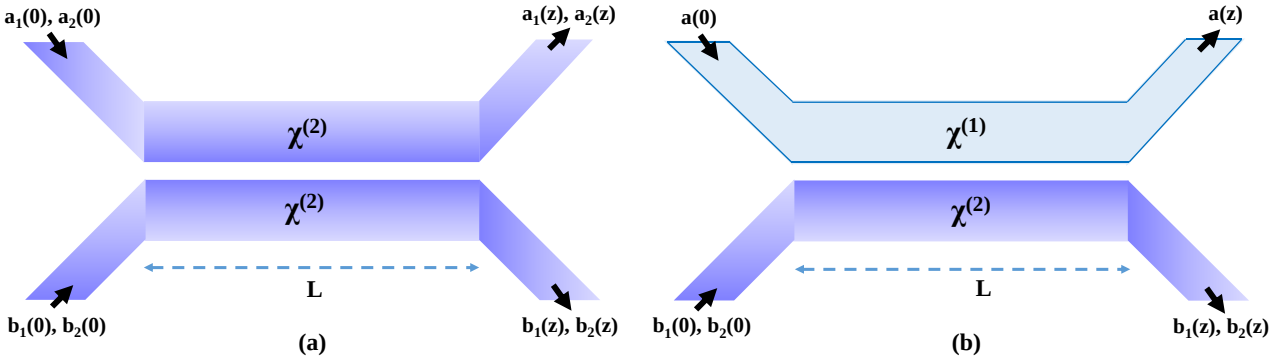

Figure 1: (Color online) Schematic diagrams of (a) a symmetric and (b) an asymmetric nonlinear optical coupler of interaction length L in a codirectional propagation of different field modes involved. The symmetric coupler is prepared by combining two nonlinear (quadratic) waveguides operating under second harmonic generation, and in the asymmetric coupler one nonlinear waveguide of the symmetric coupler is replaced by a linear waveguide.

III. LINEAR AND NONLINEAR QUANTUM ZENO AND ANTI-ZENO EFFECTS

Being consistent with the theme of the present work, the presence of quantum Zeno and anti-Zeno effects with a nonlinear probe corresponds to the nonlinear quantum Zeno and anti-Zeno effects. Similarly, a linear probe will give the linear quantum Zeno and anti-Zeno effects. Further, it has already

been mentioned in Section (1), that analytical expressions for Zeno parameter for a linear probe can be obtained as the limiting cases of the expressions obtained for nonlinear probe by neglecting the nonlinearity present in the probe [37]. Quite similar analogue of nonlinear and linear quantum Zeno and anti-Zeno effects were also discussed in the recent past [7, 38] in other physical systems.

A. Number operator and Zeno parameter

The analytic expression of the number operator for the second harmonic field mode in the system waveguide, i.e., b_2 mode using Eq. (A.2) in Appendix A is given by

$$\begin{aligned} N_{b_2}(z) &= b_2^{\dagger}(z)\, b_2(z) \\ &= b_2^{\dagger}(0)\, b_2(0) + |l_2|^2\, b_1^{\dagger 2}(0)\, b_1^2(0) + |l_3|^2\, a_1^{\dagger}(0)\, a_1(0)\, b_1^{\dagger}(0)\, b_1(0) + |l_4|^2\, a_1^{\dagger 2}(0)\, a_1^2(0) + \Big[l_2 b_2^{\dagger}(0)\, b_1^2(0) \\ &+ l_3 b_2^{\dagger}(0)\, b_1(0)\, a_1(0) + l_4 b_2^{\dagger}(0)\, a_1^2(0) + l_2^* l_3 a_1(0)\, b_1^{\dagger 2}(0)\, b_1(0) + l_2^* l_4 a_1^2(0)\, b_1^{\dagger 2}(0) + l_3^* l_4 a_1^{\dagger}(0)\, a_1^2(0)\, b_1^{\dagger}(0) \\ &+ l_5 b_1^{\dagger}(0)\, b_1(0)\, b_2^{\dagger}(0)\, b_2(0) + l_6 b_2^{\dagger}(0)\, b_2(0) + l_7 a_1(0)\, b_1^{\dagger}(0)\, b_2^{\dagger}(0)\, b_2(0) + l_8 a_1^{\dagger}(0)\, b_1(0)\, b_2^{\dagger}(0)\, b_2(0) \\ &+ l_9 a_1^{\dagger}(0)\, a_1(0)\, b_2^{\dagger}(0)\, b_2(0) + l_{10} a_1^{\dagger}(0)\, a_2(0)\, b_1(0)\, b_2^{\dagger}(0) + l_{11} a_1^{\dagger}(0)\, a_1(0)\, a_2(0)\, b_2^{\dagger}(0) + l_{12} a_2(0)\, b_2^{\dagger}(0) \\ &+ l_{13} a_2(0)\, b_1^{\dagger}(0)\, b_1(0)\, b_2^{\dagger}(0) + l_{14} a_1(0)\, a_2(0)\, b_1^{\dagger}(0)\, b_2^{\dagger}(0) + \text{H.c.} \Big], \end{aligned} \tag{3}$$

where the functional form of coefficients l_i is given in Eq. (A.3) in Appendix A.

Without any loss of generality, we considered the initial state being a multimode coherent state $|\alpha\rangle|\beta\rangle|\gamma\rangle|\delta\rangle$, which is the product of four single mode coherent states $|\alpha\rangle$, $|\beta\rangle$, $|\gamma\rangle$, and $|\delta\rangle$. Here, $|\alpha\rangle$, $|\beta\rangle$, $|\gamma\rangle$, and $|\delta\rangle$ are the eigenkets of the annihilation operators for the corresponding field modes, i.e., a_1, b_1, a_2, and b_2, respectively. For example, $b_1(0)|\alpha\rangle|\beta\rangle|\gamma\rangle|\delta\rangle = \beta|\alpha\rangle|\beta\rangle|\gamma\rangle|\delta\rangle$ and $a_1(0)|\alpha\rangle|\beta\rangle|\gamma\rangle|\delta\rangle = \alpha|\alpha\rangle|\beta\rangle|\gamma\rangle|\delta\rangle$, where $|\alpha|^2$, $|\beta|^2$, $|\gamma|^2$, and $|\delta|^2$ are the initial number of photons in the field modes a_1, b_1, a_2, and b_2, respectively. The symmetric nonlinear optical coupler and its approximated special case of the asymmetric nonlinear optical coupler can operate under two conditions: spontaneous and stimulated. In the spontaneous (stimulated) case, initially, i.e., at $t = 0$, there is no photon (non-zero number of photons) in the second-harmonic mode of the system, whereas average photon numbers in the other modes are non-zero.

Following earlier works of some of the present authors [11–15], the effect of the presence of the probe mode on the photon statistics of the second harmonic mode of the system is investigated using Zeno parameter (ΔN_Z), which is defined as

$$\Delta N_Z = \langle N_X(z)\rangle - \langle N_X(z)\rangle_{k=0}. \tag{4}$$

The Zeno parameter is a measure of the effect caused on the evolution of the photon statistics of the system (obtained for mode X) due to its interaction with the probe. It can be inferred from Eq. (4) that the negative values of the Zeno parameter signify the continuous measurement via the probe inhibited the evolution of mode X by decreasing the photon generation in that particular mode, which demonstrate presence of the quantum Zeno effect. On the other hand, the positive values of the Zeno parameter correspond to enhancement of the photon generation due to coupling with auxiliary mode in the probe. This is the signature of the presence of quantum anti-Zeno effect.

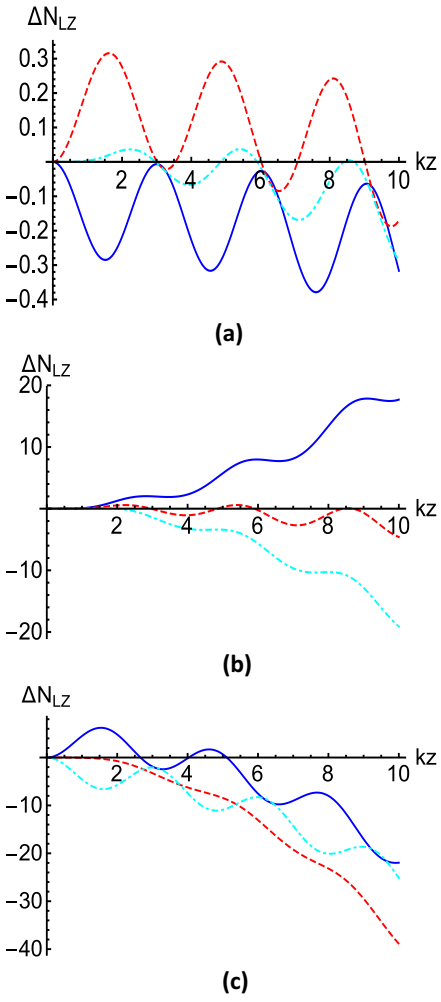

Figure 2: (Color online) (a) The variation in linear Zeno parameter with rescaled interaction length for $\frac{\Gamma_b}{k} = 10^{-2}$, $\frac{\Delta k_b}{k} = 10^{-3}$ with $\alpha = 5$, $\beta = 3$, and $\delta = 1$ and -1 in stimulated case (smooth and dashed lines) and $\delta = 0$ in spontaneous case (dot-dashed line). (b) In spontaneous case, $\alpha = 10$ with $\beta = 3, 6$, and 7 for smooth, dashed and dot-dashed lines, respectively. (c) $\alpha = 10$, $\beta = 8$, and $\delta = -4$, 0, and 4 for smooth, dashed and dot-dashed lines, respectively.

For the system of our interest, the symmetric nonlinear optical coupler, using the analytic expression of the photon number operator in Eq. (3), the Zeno parameter can be calculated for second harmonic mode of the system waveguide as

$$\begin{aligned}\Delta N_{NZ} &= \left(|l_2|^2-|p_2|^2\right)|\beta|^4+|l_3|^2|\alpha|^2|\beta|^2\\ &+ |l_4|^2|\alpha|^4+\left[(l_2-p_2)\beta^2\delta^*+l_3\alpha\beta\delta^*+l_4\alpha^2\delta^*\right.\\ &+ l_2^*l_3|\beta|^2\alpha\beta^*+l_2^*l_4\alpha^2\beta^{*2}+l_3^*l_4|\alpha|^2\alpha\beta^*\\ &+ (l_5-p_5)|\beta|^2|\delta|^2+(l_6-p_6)|\delta|^2+l_7|\delta|^2\alpha\beta^*\\ &+ l_8|\delta|^2\alpha^*\beta+l_9|\alpha|^2|\delta|^2+l_{10}\alpha^*\beta\gamma\delta^*\\ &+ l_{11}|\alpha|^2\gamma\delta^*+l_{12}\gamma\delta^*+l_{13}|\beta|^2\gamma\delta^*\\ &+ \left.l_{14}\alpha\beta^*\gamma\delta^*+\text{c.c.}\right], \end{aligned} \tag{5}$$

where

$$\begin{aligned}p_2 &= -\tfrac{\Gamma_b G_-^*}{\Delta k_b},\\ p_5 &= 2p_6=-\tfrac{4|\Gamma_b|^2\left(G_-^*+i\Delta k_b z\right)}{(\Delta k_b)^2}.\end{aligned} \tag{6}$$

Here, p_is are obtained by taking $k=0$ in corresponding l_is in Eq. (A.3) in Appendix A. All the remaining p_i's vanishes in the absence of the probe. The subscript NZ in the Zeno parameter corresponds to the physical situation where a nonlinear probe is used, i.e., "nonlinear Zeno" effect is investigated. Thus ΔN_{NZ} can be referred to as the nonlinear Zeno parameter. Similarly ΔN_{LZ} will denote linear Zeno parameter, i.e., Zeno parameter for a physical situation where linear probe is used.

It is easy to obtain Zeno parameter for the spontaneous case. Specifically, in the spontaneous case, i.e., in absence of any photon in the second harmonic mode of the system at $t=0$ (or considering $\delta=0$ at $t=0$), the analytic expression of the nonlinear Zeno parameter can be obtained from Eq. (5) by keeping the δ independent terms as

$$\begin{aligned}(\Delta N_{NZ})_{\delta=0} &= \left(|l_2|^2-|p_2|^2\right)|\beta|^4+|l_3|^2|\alpha|^2|\beta|^2\\ &+ |l_4|^2|\alpha|^4+\left[l_2^*l_3|\beta|^2\alpha\beta^*\right.\\ &+ \left.l_2^*l_4\alpha^2\beta^{*2}+l_3^*l_4|\alpha|^2\alpha\beta^*+\text{c.c.}\right].\end{aligned} \tag{7}$$

In Section II, we have already mentioned that the momentum operator for an asymmetric nonlinear optical coupler $(\chi^{(2)}-\chi^{(1)})$ can be obtained by just neglecting the nonlinear coupling term in one of the nonlinear waveguides present in the symmetric nonlinear coupler $(\chi^{(2)}-\chi^{(2)})$ studied here. Thus, we may consider the probe in the nonlinear Zeno parameter obtained in Eq. (5) to be linear by taking $\Gamma_a=0$. This is how we can obtain the expression for linear Zeno parameter. Thus, the Zeno parameter of the asymmetric nonlinear optical coupler characterized by Eq. (2) can be obtained as

$$\begin{aligned}\Delta N_{LZ} &= \left(|l_2|^2-|p_2|^2\right)|\beta|^4+|l_3|^2|\alpha|^2|\beta|^2\\ &+ |l_4|^2|\alpha|^4+\left[(l_2-p_2)\beta^2\delta^*+l_3\alpha\beta\delta^*+l_4\alpha^2\delta^*\right.\\ &+ l_2^*l_3|\beta|^2\alpha\beta^*+l_2^*l_4\alpha^2\beta^{*2}+l_3^*l_4|\alpha|^2\alpha\beta^*\\ &+ (l_5-p_5)|\beta|^2|\delta|^2+(l_6-p_6)|\delta|^2+l_7|\delta|^2\alpha\beta^*\\ &+ \left.l_8|\delta|^2\alpha^*\beta+l_9|\alpha|^2|\delta|^2+\text{c.c.}\right].\end{aligned} \tag{8}$$

Further, if we neglect all the terms beyond linear power in nonlinear coupling constant Γ_b in Eq. (8), we find the result obtained here matches exactly with the result reported in Ref. [13]. Interestingly, the analytic expressions of the nonlinear and linear Zeno parameters have the same expressions in the spontaneous case. It can also be checked that the expression obtained in Eq. (7) vanishes, if we neglect all the terms beyond linear powers in the nonlinear coupling constant. This is also consistent with the earlier result [13].

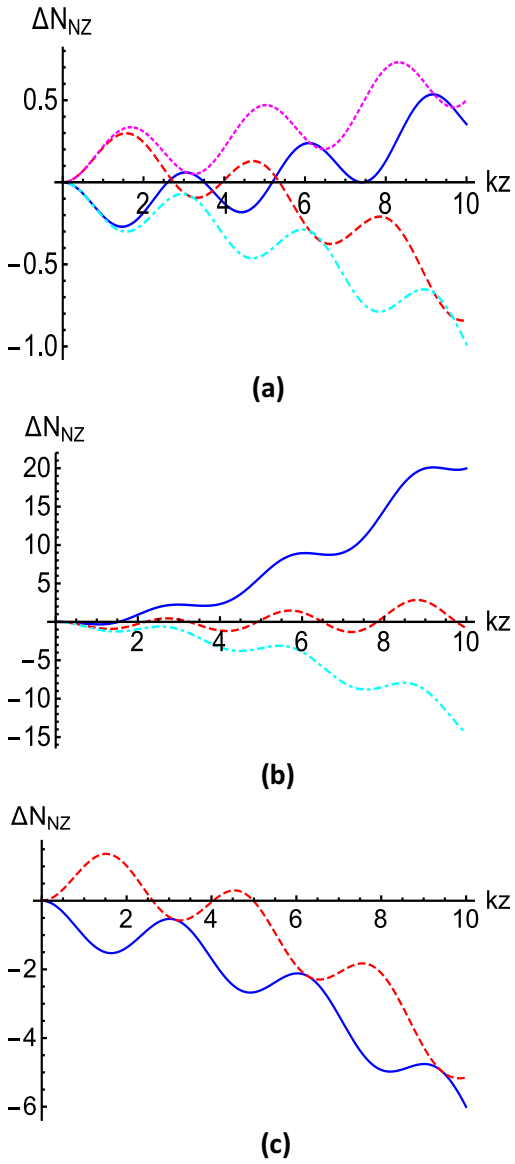

Figure 3: (Color online) (a) Nonlinear Zeno parameter with $\frac{\Gamma_a}{k}=\frac{\Gamma_b}{k}=10^{-2}$, $\frac{\Delta k_a}{k}=1.1\times10^{-3}$, $\frac{\Delta k_b}{k}=1.1\times10^{-3}$ with $\alpha=5$, $\beta=3$, and $\gamma=2$, $\delta=1$ and -1 in stimulated case (smooth and dashed lines) and $\gamma=-2$, $\delta=1$ and -1 in dot-dashed and dotted lines. (b) $\alpha=10$, $\gamma=3$, $\delta=1$ with $\beta=3,6$, and 7 for smooth, dashed and dot-dashed lines, respectively. (c) shows the change in nonlinear Zeno parameter with changing the phase of α or β by an amount of π for $\alpha=\beta=6$, and $\gamma=3$, $\delta=2$. It is also observed that the change in phase of α is equivalent to change in phase of β.

B. Variation of Zeno parameter with different variables

The analytic expressions obtained for both nonlinear and linear Zeno parameters depend on various parameters, such as photon numbers and phases of different field modes, linear and nonlinear coupling, interaction length and phase mismatch between fundamental and second harmonic modes in the nonlinear waveguides. However, in the spontaneous case, system shows quantum anti-Zeno effect initially which eventually goes towards quantum Zeno effect with increase in rescaled interaction length. This behavior of the linear Zeno parameter in the spontaneous case is further elaborated in Fig. 2 b, where it can be observed that as the number of photons in the linear mode of the system waveguide becomes comparable to the photon numbers in the probe mode, quantum Zeno effect is prominent. A similar effect on photon numbers is observed even in the stimulated case in Fig. 2 c, where the transition to quantum Zeno effect with increasing rescaled interaction length is more dominating than in Fig. 2 a. Further, in the stimulated case, a transition between linear quantum Zeno and anti-Zeno effects can be obtained by controlling the phase of second harmonic mode of the system waveguide as illustrated in Fig. 2 a. However, with an increase in number of photons in fundamental mode of the system waveguide shown in Fig. 2 c, this nature disappears gradually due to its dominant effect to tend towards quantum Zeno effect.

To illustrate the variation of the nonlinear Zeno parameter with the rescaled interaction length of the coupler in Fig. 3, we have considered specific values of all the remaining parameters. As in the case of linear Zeno parameter (cf. Fig. 2) nonlinear Zeno parameter also shows dependence on the phases of both second harmonic modes involved in the symmetric coupler. Specifically, Fig. 3 a illustrates that the change in phase of the second harmonic mode of the system creates some changes in the photon statistics which causes a transition between quantum Zeno and anti-Zeno effects. This become more dominant with the change of phase of second harmonic mode of the probe as well. Similarly, Fig. 3 b establishes an analogous fact for nonlinear Zeno parameter as in Fig. 2 b for linear Zeno parameter, i.e., when the photon numbers in the linear modes of both the waveguides are comparable then quantum Zeno effect prevails. Fig. 3 c shows that by changing the phase of α by π (i.e., transforming α to $-\alpha$) has a similar effect as changing the phase of β by the same amount. Interestingly, this kind of nature can be attributed to the symmetry present in the symmetric coupler studied here.

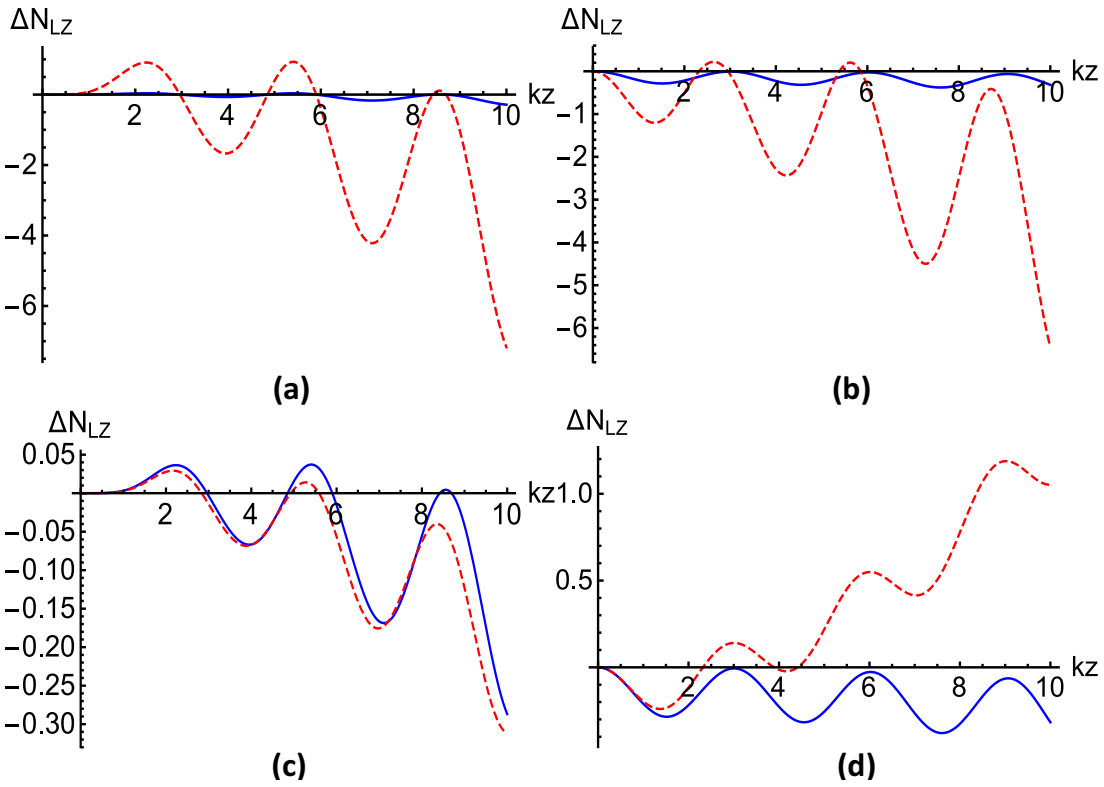

Figure 4: (Color online) (a) Linear Zeno parameter in the spontaneous case for $\frac{\Delta k_b}{k} = 10^{-3}$ with $\alpha = 5$, $\beta = 3$ for $\frac{\Gamma_b}{k} = 10^{-2}$ $\left(5 \times 10^{-2}\right)$ in smooth blue (dashed red) line. (b) A similar observation in the stimulated case with $\delta = 1$ and all the remaining values same as (a). In (c) and (d), the effect of phase mismatch in the spontaneous and stimulated (with $\delta = 1$) cases of linear Zeno parameter is shown, respectively. The remaining parameters are $\frac{\Gamma_b}{k} = 10^{-2}$ with $\frac{\Delta k_b}{k} = 10^{-3}$ $\left(10^{-1}\right)$ in the smooth blue (dashed red) line.

The explicit dependence of the linear and nonlinear Zeno parameters on the remaining parameters, such as nonlinear coupling constants and phase mismatches, of both system and probe waveguides is illustrated in Figs. 4 and 5, respectively. Specifically, Figs. 4 a-b show the variation in the linear Zeno parameter for two values of nonlinear coupling constant of the system in spontaneous and stimulated cases, respectively. A similar study is shown in Figs. 5 a-b for the nonlinear Zeno parameter with two values of nonlinear coupling constants of the system and probe waveguides, respectively. All the cases demonstrate that with increase in the nonlinear coupling of the system a dominant oscillatory nature is observed. While increase in the nonlinear coupling of the probe waveguide shows preference for quantum anti-Zeno effect.

The phase mismatch between fundamental and second harmonic modes of the system (probe) waveguide has negligible effect on the linear (nonlinear) Zeno parameter in the spontaneous (stimulated) case as depicted in Fig. 4 c (5 c). While a similar observation for linear (nonlinear) Zeno parameter shown in Fig. 4 d (5 d) for the stimulated case with phase mismatch in the system waveguide exhibits a transition from quantum Zeno effect to quantum anti-Zeno effect.

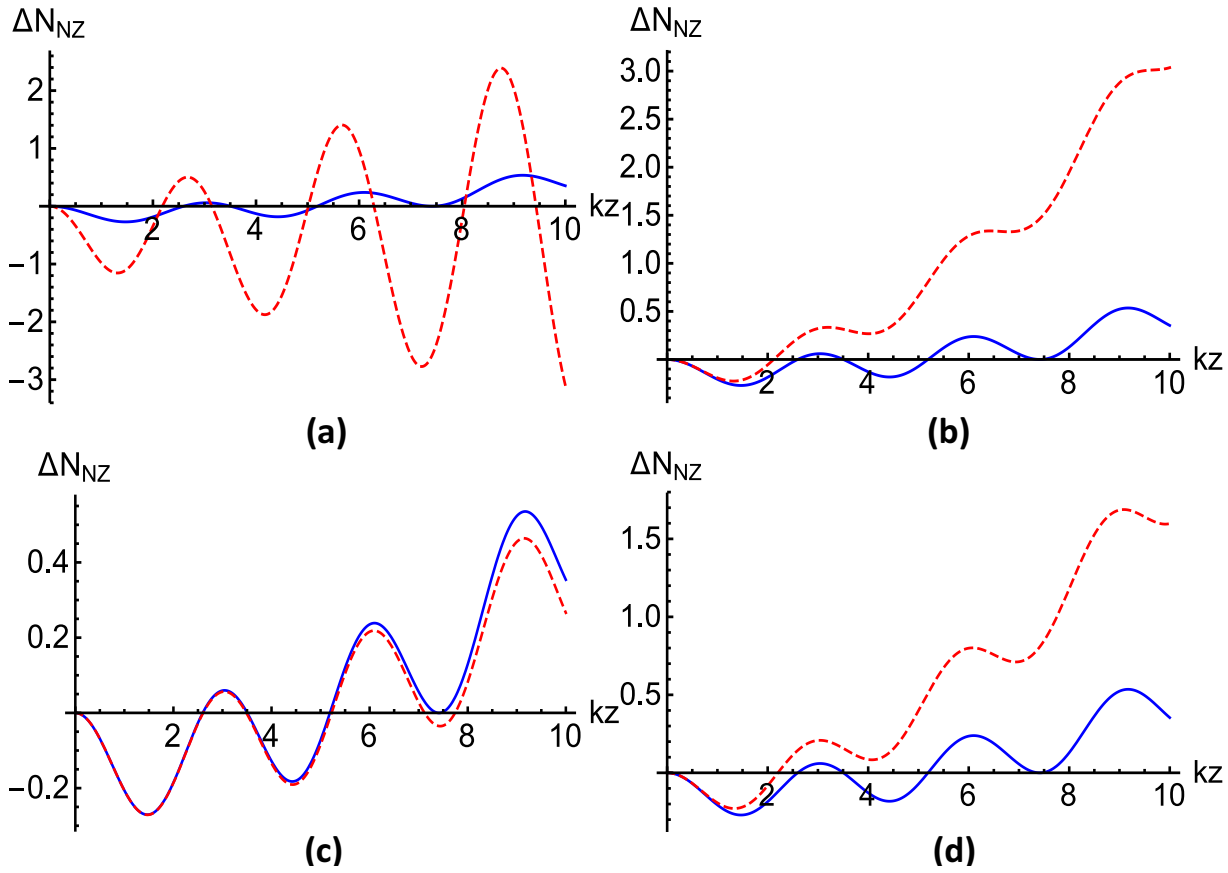

Figure 5: (Color online) The dependence of nonlinear Zeno parameter on the nonlinear coupling constant is depicted in (a) and (b). In (a) the nonlinear Zeno parameter is shown with rescaled interaction length for $\frac{\Gamma_a}{k} = 10^{-2}$, $\frac{\Delta k_a}{k} = 1.1 \times 10^{-3}$, $\frac{\Delta k_b}{k} = 10^{-3}$ with $\alpha = 5$, $\beta = 3, \gamma = 2$, and $\delta = 1$. The smooth (blue) and dashed (red) lines correspond to $\frac{\Gamma_b}{k} = 10^{-2}$ and $\frac{\Gamma_b}{k} = 5 \times 10^{-2}$, respectively. Similarly, in (b) the smooth (blue) and dashed (red) lines correspond to $\frac{\Gamma_a}{k} = 10^{-2}$ and $\frac{\Gamma_a}{k} = 5 \times 10^{-2}$, respectively with $\frac{\Gamma_b}{k} = 10^{-2}$ and all the remaining values as in (a). In (c) the nonlinear Zeno parameter is shown in the smooth blue (dashed red) line with $\frac{\Gamma_a}{k} = \frac{\Gamma_b}{k} = 10^{-2}$, $\frac{\Delta k_b}{k} = 10^{-3}$ for $\frac{\Delta k_a}{k} = 1.1 \times 10^{-3}$ $\left(1.1 \times 10^{-1}\right)$. Similarly, in (d) the nonlinear Zeno parameter is shown in the smooth blue (dashed red) line with $\frac{\Delta k_a}{k} = 1.1 \times 10^{-3}$ for $\frac{\Delta k_b}{k} = 10^{-3}$ $\left(10^{-1}\right)$.

The dependence of both linear and nonlinear Zeno parameters on the linear coupling can be observed with interaction length in Fig. 6 a and b, respectively. With the particular choice of values for other parameters, both Zeno parameters show quantum Zeno effect. However, as observed in Fig. 2 quantum anti-Zeno effect can be illustrated here by just controlling the phase of the second harmonic mode in the system. Though an increase in the effect of the presence of the probe in the photon

statistics of the second harmonic mode with increasing interaction length and linear coupling can be observed from the figure. This dominance of the effect of the probe is oscillatory in nature and gives a ripple like structure in Fig. 6.

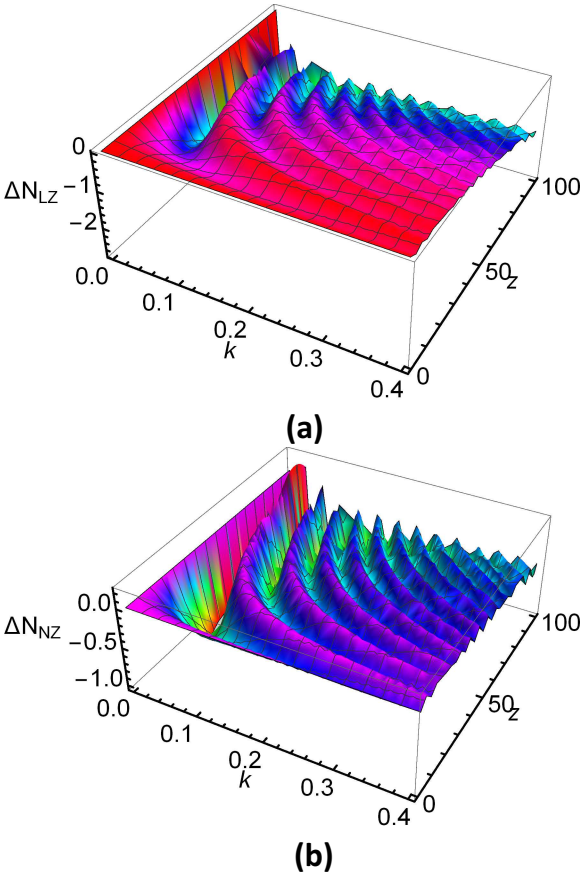

Figure 6: (Color online) The variation in (a) linear and (b) nonlinear Zeno parameter with linear coupling constant and interaction length are shown for $\frac{\Gamma_a}{k} = \frac{\Gamma_b}{k} = 10^{-2}$, $\frac{\Delta k_a}{k} = 1.1 \times 10^{-3}$, $\frac{\Delta k_b}{k} = 10^{-3}$ with $\alpha = 6$, $\beta = 4$, $\gamma = 2$, and $\delta = 1$.

The effect of change in phase mismatch between fundamental and second harmonic modes explored in Figs. 4 c-d and 5 c-d is further illustrated in Fig. 7. The phase mismatch between the fundamental and second harmonic modes in the system waveguide has evident effect on the linear Zeno parameter only in the small mismatch region for the spontaneous case (cf. Fig. 7 a). Whereas an increase in the initial number of photons in the second harmonic mode of the system, i.e., in the stimulated case, changes the photon statistics drastically and both quantum Zeno and anti-Zeno effects, with continuous switching between them, have been observed in Fig. 7 b. The corresponding plot for nonlinear Zeno parameter shows a quite similar behavior in Fig. 7 c with slight changes in the photon statistics due to the presence of the second harmonic mode in the probe. A similar study for the effect of phase mismatch between the fundamental and second harmonic modes of the probe on nonlinear Zeno parameter shows ample amount of variation only for small mismatch and becomes almost constant for larger values of phase mismatch. These features of quantum Zeno and anti-Zeno effects can be further illustrated using contour plots as shown in Fig. 8, where the values of different parameters are the same as those used in Fig. 7. The contour plots can be drawn to clearly show the regions of quantum Zeno and anti-Zeno effects (without referring to the magnitude of the Zeno parameter) as shown in Fig. 8 a and b, where the blue regions correspond to the quantum Zeno effect while the yellow regions correspond to the quantum anti-Zeno effect in the linear Zeno case. The contour plots can also be drawn to illustrate the depth of Zeno parameter for both the effects as illustrated in Fig. 8 c and d for nonlinear Zeno parameter.

Fig. 9 demonstrates the nature of linear Zeno parameter with changes in the number of photons in the linear modes of both the waveguides. Here, it can be seen that with increase in photon numbers in probe mode quantum anti-Zeno effect is preferred while with increasing the intensity in the linear mode of system waveguide it tends towards quantum Zeno effect.

IV. CONCLUSIONS

Linear and nonlinear quantum Zeno and anti-Zeno effects in a symmetric and an asymmetric nonlinear optical couplers are rigorously investigated in the present work. The investigation is performed using linear and nonlinear Zeno parameters, which are introduced in this paper in analogy with that of the Zeno parameter introduced in Ref. [13]. Closed form analytic expressions for both linear and nonlinear Zeno parameters are obtained here using Sen-Mandal perturbative method. Subsequently, variation of the Zeno and anti-Zeno parameters with respect to various quantities are investigated and the same is illustrated in Figs. 2-9. The investigation led to several interesting observations. For example, we have observed that the analytic expressions obtained for both linear and nonlinear Zeno parameters are the same for the spontaneous case. Further, in the spontaneous case, it is observed that the transition from the quantum anti-Zeno effect to quantum Zeno effect can be achieved by increasing the intensity of the radiation field in the linear mode of the system waveguide (cf. Fig. 2 b). Similarly, a switching between the linear (nonlinear) quantum Zeno and anti-Zeno effects is also observed in the stimulated case. However, it is observed that this switching can be obtained just by controlling the phase of the second harmonic mode in the system waveguide in the linear case (cf. Figs. 2 a and c) and by controlling the phase of the nonlinear modes of both the waveguides (cf. Figs. 3 a and c). Here we may note that the change in phase of the linear mode of the probe is equivalent to change in phase of the linear mode of the nonlinear system waveguide. This kind of nature can be attributed to the symmetry present in the system, which is evident even in the system momentum operator (cf. Fig. 3 c). In fact, in general, we have observed that increase in the intensity of the probe leads to increase the quantum anti-Zeno effect, while with the increase in the intensity of the linear mode of the system waveguide the quantum Zeno effect is more prominent (cf. Figs. 2 b and c and Fig. 9).

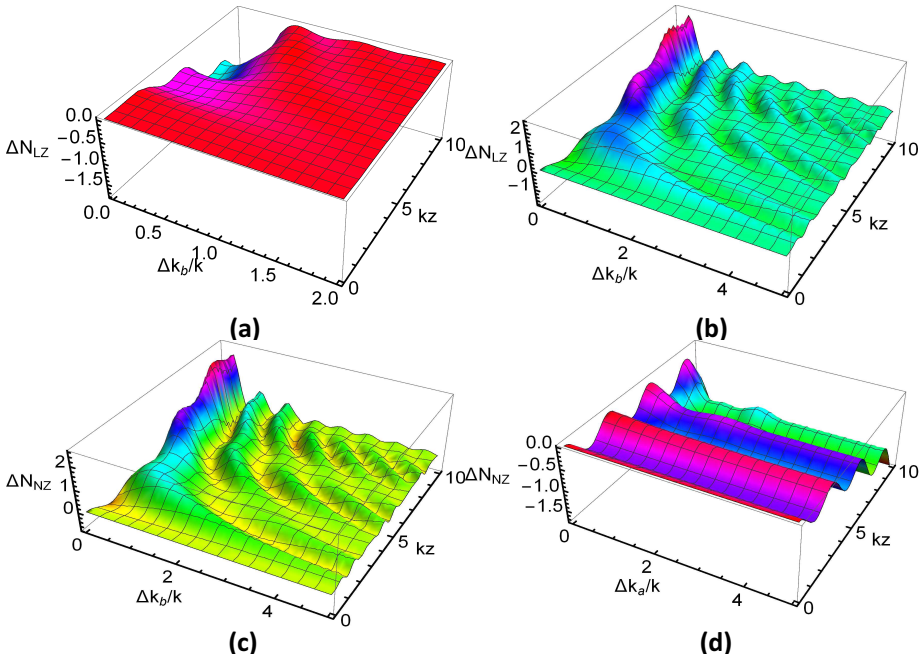

Figure 7: (Color online) The variation in linear Zeno parameter with phase mismatch between fundamental and second harmonic modes in system waveguide and rescaled interaction length in (a) spontaneous and (b) stimulated cases are shown for $\frac{\Gamma_b}{k} = 10^{-2}$ with $\alpha = 6$, $\beta = 4$, and $\delta = 0$ and 1 in (a) and (b), respectively. (c) shows the dependence of the nonlinear Zeno parameter on the phase mismatch between fundamental and second harmonic modes in system waveguide and rescaled interaction length for $\frac{\Gamma_a}{k} = 10^{-2}$, $\frac{\Delta k_a}{k} = 1.1 \times 10^{-3}$ and $\gamma = 2$, $\delta = 1$ with all remaining values same as (a) and (b). In (d), the effect of phase mismatch between fundamental and second harmonic modes in probe waveguide and rescaled interaction length on the nonlinear Zeno parameter are shown for $\frac{\Delta k_b}{k} = 10^{-3}$ with all the remaining values as (c).

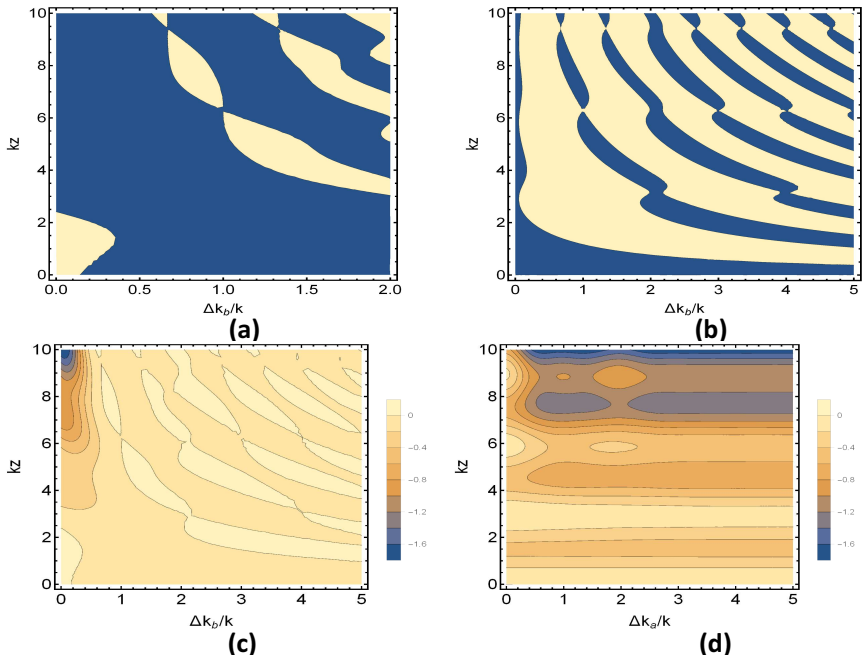

Figure 8: (Color online) Variation in linear and nonlinear Zeno parameters shown in three dimensional plots in Fig. 7 (a)-(d) are illustrated via equivalent contour plots. Here, all the four contour plots corresponding to Fig. 7 (a)-(d) are are obtained using the same parameters. In (a) and (b), the yellow regions illustrate the region for quantum anti-Zeno effect while the blue regions correspond to quantum Zeno effect. In (c) and (d), along with the regions of Zeno and anti-Zeno effects, variation of magnitude of Zeno parameters are also shown with different colors (see the color bars in right side of the figures).

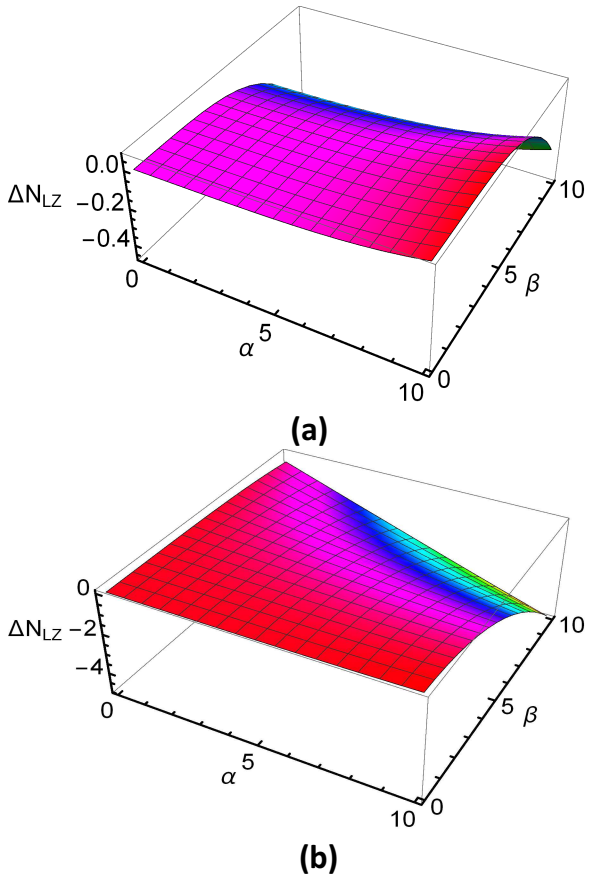

Figure 9: (Color online) The variation in linear Zeno parameter in (a) spontaneous and (b) stimulated cases with photon numbers of linear modes in both the waveguides (α and β) are shown for $\frac{\Gamma_b}{k} = 10^{-2}$, $\frac{\Delta k_b}{k} = 10^{-3}$ with $\gamma = \frac{\alpha}{2}$ and $\delta = \frac{\beta}{3}$ after rescaled interaction length $kz = 1$. A similar behavior to the linear Zeno parameter is observed for nonlinear Zeno parameter in the stimulated case.

For the smaller values of the linear coupling constant, a considerable amount of variation in the photon number statistics is observed through the linear Zeno parameter. This variation is observed to fade away as ripples with increasing interaction length for higher values of linear coupling constant (cf. Fig. 6 a). Similar but more prominent nature is observed in the nonlinear case (cf. Fig. 6 b). Similarly, we have observed that with the increase in phase mismatch between fundamental and second harmonic modes in the system waveguide, a transition from quantum Zeno effect to quantum anti-Zeno effect occurs. The change in photon number statistics of the nonlinear waveguide is more prominent in the stimulated case compared to that in the spontaneous case of linear and nonlinear Zeno parameters, respectively (cf. Fig. 7).

In brief, possibility of observing Zeno and anti-Zeno effects is rigorously investigated in symmetric and asymmetric nonlinear optical couplers, which are experimentally realizable at ease. For completely quantum description of the primary physical system (i.e., symmetric nonlinear optical coupler), appropriate use of a perturbative technique which is known to perform better than short-length method, reducibility of the results obtained for symmetric nonlinear optical coupler to that of asymmetric nonlinear optical coupler, easy experimental realizability of the physical systems, etc., provide an edge to this work over the existing works on Zeno effects in optical coupler, where usually the use of complete quantum description is circumvented by considering one or more modes as strong and/or short length method is used to reduce computational difficulty. The approach adopted here is also very general and can be easily extended to the study of other optical couplers and other quantum optical systems having the similar structure of momentum operators or Hamiltonian as is used here. We conclude the work with an expectation that the experimentalists will find this work interesting for an experimental verification and it could be possible to find its applicability in some of the recently proposed Zeno-effect-based schemes for quantum computation and communication.

Appendix A: Solution of Heisenberg's equations of motion

The solution of the momentum operator given in Eq. (1) using Sen-Mandal perturbative approach can be obtained once we write the Heisenberg's equations of motion for all the field modes involved, which are obtained as

$$\begin{aligned}
\tfrac{da_1}{dz} &= ik^* b_1 + 2i\Gamma_a^* a_1^\dagger a_2 \exp\left(-i\Delta k_a z\right), \\
\tfrac{db_1}{dz} &= ika_1 + 2i\Gamma_b^* b_1^\dagger b_2 \exp\left(-i\Delta k_b z\right), \\
\tfrac{da_2}{dz} &= i\Gamma_a a_1^2 \exp\left(i\Delta k_a z\right), \\
\tfrac{db_2}{dz} &= i\Gamma_b b_1^2 \exp\left(i\Delta k_b z\right).
\end{aligned} \tag{A.1}$$

Now, the evolution the all the field modes can be assumed up to quadratic terms in nonlinear coupling constants Γ_i in the form

$$
\begin{aligned}
a_1(z) &= f_1 a_1(0) + f_2 b_1(0) + f_3 a_1^\dagger(0) a_2(0) + f_4 a_2(0) b_1^\dagger(0) + f_5 b_1^\dagger(0) b_2(0) + f_6 a_1^\dagger(0) b_2(0) \\
&+ f_7 a_1(0) a_2^\dagger(0) a_2(0) + f_8 a_1^\dagger(0) a_1^2(0) + f_9 a_2^\dagger(0) a_2(0) b_1(0) + f_{10} a_1^\dagger(0) a_1(0) b_1(0) \\
&+ f_{11} a_1(0) b_1^\dagger(0) b_1(0) + f_{12} a_1^\dagger(0) b_1^2(0) + f_{13} a_1^2(0) b_1^\dagger(0) + f_{14} b_1^\dagger(0) b_1^2(0) \\
&+ f_{15} a_2(0) b_1(0) b_2^\dagger(0) + f_{16} a_1(0) a_2(0) b_2^\dagger(0) + f_{17} a_1(0) a_2^\dagger(0) b_2(0) \\
&+ f_{18} a_2^\dagger(0) b_1(0) b_2(0) + f_{19} b_1(0) b_2^\dagger(0) b_2(0) + f_{20} b_1^\dagger(0) b_1^2(0) + f_{21} a_1^\dagger(0) b_1^2(0) \\
&+ f_{22} a_1(0) b_2^\dagger(0) b_2(0) + f_{23} a_1(0) b_1^\dagger(0) b_1(0) + f_{24} a_1^\dagger(0) a_1(0) b_1(0) + f_{25} a_1^2(0) b_1^\dagger(0) \\
&+ f_{26} a_1^\dagger(0) a_1^2(0), \\
b_1(z) &= g_1 a_1(0) + g_2 b_1(0) + g_3 a_1^\dagger(0) a_2(0) + g_4 a_2(0) b_1^\dagger(0) + g_5 b_1^\dagger(0) b_2(0) + g_6 a_1^\dagger(0) b_2(0) \\
&+ g_7 a_1(0) a_2^\dagger(0) a_2(0) + g_8 a_1^\dagger(0) a_1^2(0) + g_9 a_2^\dagger(0) a_2(0) b_1(0) + g_{10} a_1^\dagger(0) a_1(0) b_1(0) \\
&+ g_{11} a_1(0) b_1^\dagger(0) b_1(0) + g_{12} a_1^\dagger(0) b_1^2(0) + g_{13} a_1^2(0) b_1^\dagger(0) + g_{14} b_1^\dagger(0) b_1^2(0) \\
&+ g_{15} a_2(0) b_1(0) b_2^\dagger(0) + g_{16} a_1(0) a_2(0) b_2^\dagger(0) + g_{17} a_1(0) a_2^\dagger(0) b_2(0) \\
&+ g_{18} a_2^\dagger(0) b_1(0) b_2(0) + g_{19} b_1(0) b_2^\dagger(0) b_2(0) + g_{20} b_1^\dagger(0) b_1^2(0) + g_{21} a_1^\dagger(0) b_1^2(0) \\
&+ g_{22} a_1(0) b_2^\dagger(0) b_2(0) + g_{23} a_1(0) b_1^\dagger(0) b_1(0) + g_{24} a_1^\dagger(0) a_1(0) b_1(0) + g_{25} a_1^2(0) b_1^\dagger(0) \\
&+ g_{26} a_1^\dagger(0) a_1^2(0), \\
a_2(z) &= h_1 a_2(0) + h_2 a_1^2(0) + h_3 b_1(0) a_1(0) + h_4 b_1^2(0) + h_5 a_1^\dagger(0) a_1(0) a_2(0) + h_6 a_2(0) \\
&+ h_7 a_1^\dagger(0) a_2(0) b_1(0) + h_8 a_1(0) a_2(0) b_1^\dagger(0) + h_9 a_2(0) b_1^\dagger(0) b_1(0) + h_{10} a_1(0) b_1^\dagger(0) b_2(0) \\
&+ h_{11} b_1^\dagger(0) b_1(0) b_2(0) + h_{12} b_2(0) + h_{13} a_1^\dagger(0) a_1(0) b_2(0) + h_{14} a_1^\dagger(0) b_1(0) b_2(0), \\
b_2(z) &= l_1 b_2(0) + l_2 b_1^2(0) + l_3 b_1(0) a_1(0) + l_4 a_1^2(0) + l_5 b_1^\dagger(0) b_1(0) b_2(0) + l_6 b_2(0) \\
&+ l_7 a_1(0) b_1^\dagger(0) b_2(0) + l_8 a_1^\dagger(0) b_1(0) b_2(0) + l_9 a_1^\dagger(0) a_1(0) b_2(0) + l_{10} a_1^\dagger(0) a_2(0) b_1(0) \\
&+ l_{11} a_1^\dagger(0) a_1(0) a_2(0) + l_{12} a_2(0) + l_{13} a_2(0) b_1^\dagger(0) b_1(0) + l_{14} a_1(0) a_2(0) b_1^\dagger(0).
\end{aligned}
\tag{A.2}
$$

All the f_i, g_i, h_i, and l_i can be obtained using the assumed solution (A.2) for different field modes in the coupled differential equations in Eq. (A.1) with the boundary conditions for all $F_1(z=0)=1$, where $F \in \{f, g, h, l\}$. The closed form analytic solutions given in Eq. (A.2) contain various coefficients, for example,

$$
\begin{aligned}
l_1 &= 1, \\
l_2 &= -\tfrac{\Gamma_b G_{b-}^*}{2\Delta k_b} + \tfrac{iC_b}{2}\left[2|k|\left(G_{b+}^* - 1\right)\sin 2|k|z - i\Delta k_b\right. \\
&\times \left.\left(1 - \left(G_{b+}^* - 1\right)\cos 2|k|z\right)\right], \\
l_3 &= \tfrac{-C_b|k|\left[i\Delta k_b\left(G_{b+}^*-1\right)\sin 2|k|z + 2|k|\left(1-\left(G_{b+}^*-1\right)\cos 2|k|z\right)\right]}{k^*}, \\
l_4 &= \tfrac{\Gamma_b|k|^2 G_{b-}^*}{2k^{*2}\Delta k_b} + \tfrac{iC_b|k|^2}{2k^{*2}}\left[2|k|\left(G_{b+}^* - 1\right)\sin 2|k|z - i\Delta k_b\right. \\
&\times \left.\left(1 - \left(G_{b+}^* - 1\right)\cos 2|k|z\right)\right], \\
l_5 &= \tfrac{|C_b|^2}{|k|\Delta k_b^2}\left[-16|k|^5\left(G_{b-}^* + i\Delta k_b z\right) - 8i|k|^4\Delta k_b G_{b-}^*\right. \\
&\times \sin 2|k|z + 6i|k|^2\Delta k_b^3 G_{b-}^* \sin 2|k|z - i\Delta k_b^5 \sin 2|k|z \\
&+ 4|k|^3\Delta k_b^2\left(\cos 2|k|z - 1 + 3G_{b-}^* + 3i\Delta k_b z\right) + \Delta k_b^4 \\
&\times \left.|k|\left(\left(1 - 2G_{b-}^*\right)\cos 2|k|z - 1 - 2G_{b-}^* - 2i\Delta k_b z\right)\right], \\
l_6 &= \tfrac{|C_b|^2}{\Delta k_b^2}\left[-16|k|^4\left(G_{b-}^* + i\Delta k_b z\right) - 4i|k|\Delta k_b^3\right. \\
&\times \left(G_{b+}^* - 1\right)\sin 2|k|z + 4|k|^2\Delta k_b^2 \\
&\times \left(\cos 2|k|z\left(G_{b+}^* - 1\right) + 2G_{b-}^* - 1 + 3i\Delta k_b z\right) \\
&+ \left.\Delta k_b^4\left(\cos 2|k|z\left(G_{b+}^* - 1\right) - 1 - G_{b-}^* - 2i\Delta k_b z\right)\right], \\
l_7 &= \tfrac{|C_b|^2}{k^*\Delta k_b}\left[2\Delta k_b^4 \sin^2|k|z + 4i|k|^3\Delta k_b \sin 2|k|z\right. \\
&- i|k|\Delta k_b^3\left(2G_{b-}^* - 1\right)\sin 2|k|z \\
&+ 8|k|^4\left(-G_{b-}^*\cos 2|k|z + G_{b-}^* - i\Delta k_b z\right) \\
&+ \left.2|k|^2\Delta k_b^2\left(3G_{b-}^*\cos 2|k|z - G_{b-}^* + i\Delta k_b z\right)\right], \\
l_8 &= -\tfrac{|C_b|^2}{k\Delta k_b}\left[2\Delta k_b^4 \sin^2|k|z - i|k|\Delta k_b^3 \sin 2|k|z\right. \\
&+ 4i|k|^3\Delta k_b\left(2G_{b-}^* - 1\right)\sin 2|k|z \\
&+ 8|k|^4\left(-G_{b-}^*\cos 2|k|z + G_{b-}^* + i\Delta k_b z\right) + 2|k|^2 \\
&\times \left.\Delta k_b^2\left(\left(G_{b+}^* + 2\right)\cos 2|k|z - G_{b-}^* - 4 - i\Delta k_b z\right)\right], \\
l_9 &= \tfrac{|C_b|^2}{|k|\Delta k_b^2}\left[-16|k|^5\left(G_{b-}^* + i\Delta k_b z\right) + \left\{8i|k|^4\Delta k_b G_{b-}^*\right.\right. \\
&- 2i|k|^2\Delta k_b^3\left(G_{b+}^* + 2\right) + \left.i\Delta k_b^5\right\}\sin 2|k|z + 4|k|^3 \\
&\times \left(\left(1 - 2G_{b-}^*\right)\cos 2|k|z - 1 + G_{b-}^* + 3i\Delta k_b z\right) \\
&\times \left.\Delta k_b^2 + |k|\Delta k_b^4\left(\cos 2|k|z - 1 - 2i\Delta k_b z\right)\right], \\
l_{10} &= \tfrac{2C_{ab}|k|\left(G_{ab+}-1\right)}{k^*}\left[2i|k|^2\Delta k_b\Delta k_{ab}\sin 2|k|z\left\{4|k|^2\right.\right. \\
&\times \left(\Delta k_b\left(G_{a-}^* - 1\right) - \Delta k_a\left(G_{a-}^* + 1\right) + \Delta k_b\right) \\
&- \left(\Delta k_b^2\left(\Delta k_b - 2\Delta k_a\right) + \left(\Delta k_{ab}^3 - 2\Delta k_a^2\Delta k_b\right)\right. \\
&\times \left.\left.\left(G_{a-}^* - 1\right)\right)\right\} - i\Delta k_a^2\Delta k_b^2\Delta k_{ab}^3\left(G_{a+}^* - 1\right) \\
&\times \sin 2|k|z + 16|k|^5\left(-\Delta k_b\Delta k_{ab}G_{a-}^*\cos 2|k|z\right. \\
&+ \left(\Delta k_a\left(G_{ab-}^* - 1\right) + \Delta k_{ab}\left(G_{a+}^* - 1\right) + \Delta k_b\right) \\
&\times \Delta k_a) - 4|k|^3\left\{\Delta k_b\Delta k_{ab}\cos 2|k|z\right. \\
&\times \left(\Delta k_a^2\left(3G_{a+}^* - 2\right) - \Delta k_a\Delta k_b G_{a+}^* - \Delta k_b^2 G_{a-}^*\right) \\
&+ \Delta k_a\left(\left(\Delta k_b^2\Delta k_{ab} + \Delta k_{ab}^3\right)\left(G_{a+}^* - 1\right)\right. \\
&+ \Delta k_b^3 + \Delta k_b\Delta k_{ab}^2 - \left(G_{ab+}^* - 1\right) \\
&\times \left.\left.\left(2\Delta k_a^2\Delta k_b - 4\Delta k_a\Delta k_b^2 + \Delta k_a^3 + 2\Delta k_b^3\right)\right)\right\} \\
&- |k|\Delta k_a\Delta k_b\Delta k_{ab}^2\left(\Delta k_b\Delta k_{ab}\left(G_{a-}^* - 1\right)\right. \\
&+ 2\Delta k_a^2\left(G_{ab+}^* - 1\right) - \Delta k_b^2 + \cos 2|k|z\left(-\Delta k_b^2\right. \\
&+ \left.\left.\left.\left(\Delta k_a\Delta k_b - 2\Delta k_a^2 + \Delta k_b^2\right)\left(G_{a+}^* - 1\right)\right)\right)\right],
\end{aligned}
$$

$$
\begin{aligned}
l_{11} &= -\tfrac{2C_{ab}k(G_{ab+}-1)}{k^*}\left[32|k|^6\left(\Delta k_a\left(G^*_{ab-}-1\right)+\Delta k_b\right.\right.\\
&+ \left.\Delta k_{ab}\left(G^*_{a+}-1\right)\right)+16i\Delta k_b\Delta k_{ab}|k|^5G^*_{a-}\sin 2|k|z\\
&- 2\Delta k_a^2\Delta k_b^2\Delta k_{ab}^3\left(G^*_{a+}-1\right)\sin^2|k|z+\{4i\Delta k_b\Delta k_{ab}\\
&\times |k|^3\left(-\Delta k_a\Delta k_bG^*_{a+}-\Delta k_b^2G^*_{a-}+\Delta k_a^2\left(3G^*_{a+}-2\right)\right)\\
&- i\Delta k_a\left(\Delta k_b^2+\left(2\Delta k_a^2-\Delta k_a\Delta k_b-\Delta k_b^2\right)\left(G^*_{a+}-1\right)\right)\\
&\times \left.\Delta k_b\Delta k_{ab}^2|k|\right\}\sin 2|k|z-8|k|^4\left\{\Delta k_b\Delta k_{ab}\cos 2|k|z\right.\\
&\times \left(\Delta k_bG^*_{a-}-\Delta k_a\left(G^*_{a-}+1\right)\right)-\Delta k_a\left(G^*_{ab+}-1\right)\\
&\times \left(\Delta k_a\Delta k_b+3\Delta k_{ab}^2\right)+\Delta k_b\left(\Delta k_{ab}^2+\Delta k_b^2\right)+\left(G^*_{a+}\right.\\
&- \left.1\right)\left(-5\Delta k_a^2\Delta k_b+4\Delta k_a\Delta k_b^2+3\Delta k_a^3-2\Delta k_b^3\right)\}\\
&+ 2\Delta k_{ab}|k|^2\left\{\Delta k_b\left(\Delta k_b^2\left(\Delta k_b-2\Delta k_a\right)+\left(G^*_{a+}-1\right)\right.\right.\\
&\times \left.\left(\Delta k_{ab}^3-2\Delta k_a^2\Delta k_b\right)\right)\cos 2|k|z+\Delta k_a^3\left(G^*_{ab-}+1\right)\\
&\times \left(2\Delta k_{ab}-\Delta k_b\right)+\Delta k_b^3\Delta k_{ab}+\left(G^*_{a+}-1\right)\\
&\times \left.\left(2\Delta k_a^2\Delta k_{ab}^2-2\Delta k_a\Delta k_b^3+3\Delta k_a^2\Delta k_b^2+\Delta k_b^4\right)\right\}\Big],\\
l_{12} &= \tfrac{-2C_{ab}k(G_{ab+}-1)\left(4|k|^2-\Delta k_{ab}^2\right)}{k^*}\left[8|k|^4\left(\Delta k_a\left(G^*_{ab-}-1\right)\right.\right.\\
&+ \left.\Delta k_{ab}\left(G^*_{a+}-1\right)+\Delta k_b\right)+\Delta k_a^2\Delta k_b^2\Delta k_{ab}\sin^2|k|z\\
&\times \left(G^*_{a+}-1\right)-2|k|^2\left\{\Delta k_a\Delta k_{ab}\left(G^*_{a+}-1\right)\cos 2|k|z\right.\\
&\times \Delta k_b+\Delta k_{ab}\left(\Delta k_a^2+\Delta k_b^2\right)\left(G^*_{a+}-1\right)+\Delta k_a^3\\
&\times \left.\left(G^*_{a-}-1\right)\Delta k_b^3\right\}+i\Delta k_a\Delta k_b|k|\left(\Delta k_a^2-\Delta k_b^2\right)\\
&\times \left.\left(G^*_{a+}-1\right)\sin 2|k|z\right],\\
l_{13} &= \tfrac{-2C_{ab}k|k|(G_{ab+}-1)}{k^*}\left[32|k|^5\left(\Delta k_a\left(G^*_{ab-}-1\right)+\Delta k_b\right.\right.\\
&+ \left.\Delta k_{ab}\left(G^*_{a+}-1\right)\right)-4i\Delta k_b\Delta k_{ab}|k|^2\sin 2|k|z\\
&\times \left\{4|k|^2G^*_{a-}-\Delta k_a\Delta k_b\left(3G^*_{a+}-2\right)+\Delta k_a^2G^*_{a+}\right.\\
&- \left.\Delta k_b^2G^*_{a-}\right\}-i\Delta k_a\Delta k_b^2\Delta k_{ab}^2\sin 2|k|z\\
&\times \left(-\Delta k_b+\Delta k_{ab}\left(G^*_{a+}-1\right)\right)-8|k|^3\left\{\Delta k_b\Delta k_{ab}\right.\\
&\times \left(-\Delta k_bG^*_{a-}+\Delta k_a\left(G^*_{a+}+1\right)\right)\cos 2|k|z\\
&- \Delta k_{ab}\left(G^*_{ab+}-1\right)\left(\Delta k_a^2+\Delta k_b\Delta k_{ab}\right)\\
&+ \left.\left(\Delta k_b+\Delta k_{ab}\left(G^*_{a+}-1\right)\right)\left(\Delta k_b^2+\Delta k_{ab}^2\right)\right\}\\
&- 2\Delta k_b\Delta k_{ab}|k|\left\{\cos 2|k|z\left(-\Delta k_b^2\left(\Delta k_a+\Delta k_{ab}\right)\right.\right.\\
&- \left.\Delta k_{ab}^2\left(\Delta k_a+\Delta k_b\right)\left(G^*_{a+}-1\right)\right)-\Delta k_b\Delta k_{ab}^2\\
&\times \left.\left(G^*_{a+}-1\right)+\Delta k_a^3\left(G^*_{ab+}-1\right)-\Delta k_b^2\Delta k_{ab}\right\}\Big],\\
l_{14} &= \tfrac{-2C_{ab}k^2(G_{ab+}-1)}{k^*}\left[2\Delta k_a\Delta k_b^2\Delta k_{ab}^2\left(-\Delta k_b+\Delta k_{ab}\right.\right.\\
&\times \left.\left(G^*_{a+}-1\right)\right)+2i\Delta k_b\Delta k_{ab}|k|\sin 2|k|z\left\{-4|k|^2\right.\\
&\times \left(-\Delta k_bG^*_{a-}+\Delta k_a\left(G^*_{a+}+1\right)\right)+\left(\Delta k_a+\Delta k_{ab}\right)\\
&\times \left.\Delta k_b^2+\Delta k_{ab}^2\left(\Delta k_a+\Delta k_b\right)\left(G^*_{a+}-1\right)\right\}+16|k|^4\\
&\times \left\{-\Delta k_b\Delta k_{ab}G^*_{a-}\cos 2|k|z+\Delta k_a\left(\left(G^*_{a+}-1\right)\right.\right.\\
&\times \left.\Delta k_{ab}+\left(\left(\Delta k_b-\Delta k_{ab}\right)\left(G^*_{ab+}-1\right)-\Delta k_b\right)\right\}\\
&- 4|k|^2\left\{\Delta k_b\Delta k_{ab}\left(-\Delta k_a\Delta k_b\left(3G^*_{a+}-2\right)-\Delta k_b^2\right.\right.\\
&\times \left.G^*_{a-}+\Delta k_a^2G^*_{a+}\right)\cos 2|k|z+\Delta k_a\left(\left(\Delta k_b-\Delta k_{ab}\right)\right.\\
&\times \Delta k_a^2\left(G^*_{ab+}-1\right)+\left(\Delta k_b^2+\Delta k_{ab}^2\right)\left(-\Delta k_b\right.\\
&+ \left.\left.\left.\left.\Delta k_{ab}\left(G^*_{a+}-1\right)\right)\right)\right\}\Big] \qquad \text{(A.3)}
\end{aligned}
$$

with $G_{i\pm} = (1\pm\exp(-i\Delta k_i z))$ for $i \in \{a,b,ab\}$, and $\Delta k_{ab} = \Delta k_a - \Delta k_b$. Also, $C_a = \frac{\Gamma_a}{[4|k|^2-\Delta k_a^2]}$, $C_b = \frac{\Gamma_b}{[4|k|^2-\Delta k_b^2]}$ and $C_{ab} = \frac{\Gamma_a^*\Gamma_b}{\Delta k_a\Delta k_b\Delta k_{ab}[4|k|^2-\Delta k_a^2][4|k|^2-\Delta k_b^2][4|k|^2-\Delta k_{ab}^2]}$.

Acknowledgement: J P thanks Project LO1305 of the Ministry of Education, Youth and Sports of the Czech Republic.

[1] L. A. Khalfin, Dokl. Akad. Nauk SSSR **115**, 277 (1957) [Sov. Phys. Dokl. **2**, 232 (1958)]; Zh. Eksp. Teor. Fiz. **33**, 1371 (1958) [Sov. Phys. JETP **6**,1053 (1958)]; Dokl. Akad. Nauk SSSR **141**, 599 (1961) [Sov. Phys. Dokl. **6**, 1010 (1962)].

[2] B. Misra and E. C. G. Sudarshan, J. Math. Phys. **18**, 756-763 (1977).

[3] A. Venugopalan, Resonance **12**, 52-68 (2007).

[4] P. Facchi and S. Pascazio, in *Quantum Zeno and Inverse Quantum Zeno Effects*, edited by E. Wolf, Progress in Optics Vol. 42 (Elsevier, Amsterdam, 2001), pp. 147-218.

[5] S. Pascazio, Open Systems and Information Dynamics **21**, 1440007 (2014).

[6] P. Facchi, and S. Pascazio, Three different manifestations of the quantum Zeno effect. Lecture notes in Physics **622**, 141-156 (2003).

[7] F. K. Abdullaev, V. V. Konotop, and V. S. Shchesnovich, Phys. Rev. A **83**, 043811 (2011).

[8] K. Thapliyal, A. Pathak, B. Sen, and J. Peřina, Phys. Rev. A **90**, 013808 (2014).

[9] K. Thapliyal, A. Pathak, B. Sen, and J. Peřina, Phys. Lett. A

378, 3431-3440 (2014).
[10] J. Peřina Jr. and J. Peřina, in *Quantum Statistics of Nonlinear Optical Couplers*, edited by E. Wolf, Progress in Optics **41**, 361-419 (Elsevier, Amsterdam, 2000).
[11] J. Řeháček, J. Peřina, P. Facchi, S. Pascazio, and L. Mišta Jr, Opt. Spectrosc. **91**, 501-507 (2001).
[12] K. Thun, J. Peřina, and J. Křepelka, Phys. Lett. A **299**, 19-30 (2002).
[13] K. Thapliyal and A. Pathak, Proceedings of International Conference on Optics and Photonics, February 20-22, Kolkata, India , Proc. of SPIE **9654**, 96541F1-96541F7 (2015).
[14] L. Mišta Jr, V. Jelínek, J. Rehácek, and J. Peřina, J. Opt. B: Quantum Semiclassical Opt. **2**, 726 (2000).
[15] J. Řeháček, J. Peřina, P. Facchi, S. Pascazio, and L. Mišta, Phys. Rev. A **62**, 013804 (2000).
[16] A. Luis and J. Peřina, Phys. Rev. Lett. **76**, 4340 (1996).
[17] A. Luis and L. L. Sánchez-Soto, Phys. Rev. A **57**, 781 (1998).
[18] J. Řeháček, J. Peřina, P. Facchi, S. Pascazio, and L. Mišta, Phys. Rev. A **62**, 013804 (2000).
[19] J. Peřina, Phys. Lett. A **325**, 16-20 (2004).
[20] G. S. Agarwal and S. P. Tewari, Phys. Lett. A **185**, 139-142 (1994).
[21] P. G. Kwiat, A. G. White, J. R. Mitchell, O. Nairz, G. Weihs, H. Weinfurter, and A. Zeilinger, Phys. Rev. Lett. **83**, 4725 (1999).
[22] W. M. Itano, D. J. Heinzen, J. J. Bollinger, and D. J. Wineland, Phys. Rev. A **41**, 2295 (1990).
[23] M. C. Fischer, B. Gutiérrez-Medina, and M. G. Raizen, Phys. Rev. Lett. **87**, 040402 (2001).
[24] O. Hosten, M. T. Rakher, J. T. Barreiro, N. A. Peters, and P. G. Kwiat, Nature **439**, 949-952 (2006).
[25] H. Salih, Z. H. Li, M. Al-Amri, and M. S. Zubairy, Phys. Rev. Lett. **110**, 170502 (2013).
[26] P. Facchi, Z. Hradil, G. Krenn, S. Pascazio, and J. Řeháček, Phys. Rev. A **66**, 012110 (2002).
[27] S. Pascazio, P. Facchi, Z. Hradil, G. Krenn, and J. Rehacek, Fortschritte der Physik **49**, 1071-1076 (2001).
[28] H. Nikolić, Phys. Lett. B **733**, 6-10 (2014).
[29] D. A. Zezyulin, V. V. Konotop, G. Barontini, and H. Ott, Phys. Rev. Lett. **109**, 020405 (2012).
[30] A. Beige, D. Braun, B. Tregenna, and P. L. Knight, Phys. Rev. Lett. **85**, 1762 (2000).
[31] A. Tavakoli, H. Anwer, A. Hameedi, and M. Bourennane, Phys. Rev. A **92**, 012303 (2015).
[32] S. Mandal and J. Peřina, Phys. Lett. A **328**, 144-156 (2004).
[33] J. Peřina and J. Peřina Jr, Quantum Semiclassical Opt. **7**, 849 (1995).
[34] J. Peřina and J. Peřina Jr, J. Modern Opt. **43**, 1951-1971 (1996).
[35] V. Peřinová, A. Lukš, and J. Křepelka, Physica Scripta **2011**, 014020 (2011).
[36] A. Luks and V. Perinová, *Quantum Aspects of Light Propagation* (Springer, New York, 2009) p. 114.
[37] W.D. Li and J. Liu, Phys. Rev. A **74**, 063613 (2006).
[38] V. S. Shchesnovich and V. V. Konotop, Phys. Rev. A **81**, 053611 (2010).